Mikrovågsavbildning för Mammografi

Magnus Otterskog*

20 januari 2007

***Mälardalens högskola, Institutionen för Datavetenskap och Elektronik**

Mikrovågsavbildning för Mammografi

Denna rapport är en del av examinationen i kursen med samma namn som titeln och består i att besvara ett antal uppgifter.

Uppgift 1 går ut på att förklara skillnader och likheter mellan röntgenmammografi och fyra av de möjliga ersättnings- eller kompletteringsmetoder som det bedrivs forskning på idag. Alla dessa fyra är modellbaserade tekniker och finns beskrivna i boken ”Alternative Breast Imaging – Four Model-Based Approaches” som är skriven av Paulsen, Meaney och Gilman. Denna bok har använts för att inhämta kunskap om de olika metoderna och besvara frågeställningen i uppgift 1.

Uppgift 2 förklarar ”unwrapping of phase” som Meany m.fl. har presenterat i sin artikel ”Microwave Image Reconstruction Utilizing Log-Magnitude and Unwrapped Phase to Improve High-Contrast Object Recovery”. Uppgiften innehåller simuleringsresultat från Qwed och Matlab.

Uppgift 3 förklarar skillnaderna mellan Paulsen och Meaneys angreppsmetod och Semenovs resp. Hagness angreppsmetoder. Vilka likheter och skillnader finns?

Uppgift 4 ger några förslag på hur man skulle kunna designa en mikrovågstomograf för att förbättra de system som finns idag samt några nya idéer på hårdvarulösningar som är värda att undersöka vidare.

Svaren är på engelska p.g.a. den stora mängd engelska termer som används i kurslitteraturen vilka, i många fall, är svåra att försvenska.

Uppgift 1

X-ray Mammography is the technological device that is used to detect cancer tumours in breasts. The technology uses X-rays that are transmitted through the breast and detected, either digitally or with ”X-ray film”, on the opposite side of the object. The X-rays are not scattered nor diffracted inside the breast and travels in straight lines through the breast which makes it very easy to locate any abnormalities. Unfortunately the technology has some drawbacks:

- The false negative and false positive rates are very high. This is mostly due to the fact that the X-ray contrast of the cancer tissue is quite low with respect to the healthy breast tissue.
- Since the radiographical density in healthy breast tissue can vary from individual to individual and also from time to time on the same individual the sensitivity will vary between measurements. Unfortunately the X-ray mammography is less sensitive in finding tumours in women with radiographically dense breasts and since this group of women represent a higher risk group due to this dense tissue probability the problem is severe.
- Often the women experience discomfort due to the breast compression that is needed during examination.
- Finally the X-rays are ionizing radiation and can induce cancer.

All these drawbacks with the X-ray mammography encourage the development of alternative or at least complementing detection methods.

Four technologies are explained in the book:

MRE – Magnetic Resonance Elastography
EIS – Electrical Impedance Spectroscopy
MIS – Microwave Imaging Spectroscopy
NIS – Near Infrared Spectroscopy Imaging

All of these are model based and uses both measurements and computer simulations and calculations. The measurements are compared with the computer simulation results and the computer model is updated (optimized) until the measurements and the computer simulations show the same results. Now a tomographic image of the object is available in the optimized computer simulation model. In this book the Finite Element Method (FEM) is used for computer simulations in all four methods. The optimization process, that tries to find the correct distribution of material parameters inside the object to obtain the measured field quantities outside the object, is a non-linear optimization process. The non-linearity is due to the fact that the material parameters have a non-linear relationship to the field solutions that they create outside the object. This is dependent on the fact that all four technologies uses waves that are diffracted and scattered by the objects inside the imaging object and this creates a non-linear dependency between the measured fields and the material parameter distribution. As a comparison the X-rays only move in straight lines through the object and only the objects that are in the linear path between the transmitter and receiver will affect the measurement results. The book uses an iterative Gauss Newton method to solve the non-linear optimization problem.

MRE – Magnetic Resonance Elastography

Low frequency, mechanical vibrations are applied to the target and the spatial displacements are measured within it by means of phase-contrast magnetic resonance imaging (MRI). Harmonic displacements within the domain of interest are measured in phase with the mechanical excitation and compared to displacements calculated using the numerical computer model of the elastic-property distribution within the target volume. The large computational power needed for a MRE calculation has led to division of the volume into subvolumes and calculations on parallel processors. The mechanical actuators used in their system are based on piezoelectric crystals. Motion is induced by coupling the actuator to the lower surface of the tissue. The piezoelectric actuators are driven by a 150 V (p-p) sinusoidal voltage with a fixed frequency, typically less than 300 Hz. The signal is produced by a signal generator, phase locked to the 10 MHz reference clock of the MR-system, and an amplifier. This produces displacements on the surface of the tissue on the order of 40 μm but larger displacements are obtained inside the breast due to constructive interference of multiple wave propagation in different directions. Several MRI displacement estimation schemes have been proposed for measuring tissue motion. These techniques include spatial magnetization tagging, simulated echo imaging and phase-contrast imaging and the latter is used in their system. The premise of phase-contrast MRI is that phase changes will arise when the motion of excited protons occurs in the presence of a magnetic field gradient. The net phase change $\phi(t)$, incurred over time t from 0 to T when a spin with position vector $\mathbf{r}(t)$ is in the presence of gradient $\mathbf{G}(t)$ is given by (1).

$$\phi(t) = \gamma \int_0^T \mathbf{G}(t) \cdot \mathbf{r}(t) dt \quad (1)$$

γ is the gyro magnetic ratio for the spin. It relates the spin's resonance frequency ω to the strength of the local magnetic field B_0 by $\omega=\gamma B_0$. For a uniform velocity v(t), the position of excited spins is given by (2).

$$\mathbf{r}(t) = \mathbf{r}_0 + v(t) \quad (2)$$

Where $\mathbf{r}_0$ is the location of the spin at time t=0. (1) and (2) gives (3).

$$\phi = \gamma \int_0^T \mathbf{G}(t) \cdot \mathbf{r}_0 dt + \int_0^T \mathbf{G}(t) \cdot \mathbf{v}(t) dt \quad (3)$$

From (3) we see that the phase change will occur both for stationary spins and for moving spins. In general, the phase changes due to the stationary spins are used for normal MR images, however, in elastographic imaging only the accumulation associated with moving spins are of interest. The phase accumulation associated with stationary spins is eliminated acquiring the MR signal in phase-cycling mode i.e. the net phase is computed from the average of two acquisitions that are obtained with opposite motion encoding gradients. For the situation where spins are undergoing simple harmonic motion, the displacement of spins at equilibrium position $\mathbf{r}_0$ is given by (4).

$$\xi(\mathbf{r}, \theta) = \mathbf{r}_0 + \xi_0 \cos(k_r \mathbf{r} - \omega t + \theta) \quad (4)$$

ξ_0 and ω are the amplitude and angular frequency of vibration, respectively, k_r is the wave number and θ is the initial phase offset between the motion encoding MR gradient and the mechanical excitation. A phase accumulation can also be generated through the MR field of view by applying an oscillating gradient $\mathbf{G}(t) = \mathbf{G}_0 \cdot \cos(\theta - \omega t)$ to the tissue for a duration T. The phase accumulation resulting from a particle undergoing simple harmonic motion is given by (5).

$$\phi(\mathbf{r}, \theta) = \gamma \int_0^T \mathbf{G}_0 \cdot \xi_0 \cdot \cos(k_r \mathbf{r} - \omega t + \theta) dt = \frac{2\gamma NT(\mathbf{G}_0 \cdot \xi_0)}{\pi} \cdot \sin(k_r \mathbf{r}) \quad (5)$$

N is the number of gradient cycles in the interval T. Snapshots of the propagating wave front are obtained as function of time by varying the initial phase offset between the motion encoding gradient and the mechanical actuator. The figure below illustrates the above mentioned method.

Experiments on simple phantoms have been performed and the following figure shows the relation between the lesion contrast and its size for detection and characterization. Also a preliminary clinical evaluation has been performed on healthy breasts and compared with images obtained from MR tomography.

EIS – Electrical Impedance Spectroscopy

In EIS, electrodes are placed in contact with the object and voltages or currents are applied. The induced voltages or currents are measured by the same electrodes and an estimation of the internal distribution of the conductivity and permittivity in the domain is done. The frequencies range from 1 kHz to 10 MHz. Like the rest of the other modalities the system uses an iterative image reconstruction approach based on FE (finite element) modelling. The book refers to Surowiec et al, that shows that the conductivity and permittivity of breast carcinoma has a contrast of up to 1:10 compared with normal breast tissue at these frequencies. The calculations are built on Maxwell's equations (ME) (6) and (7).

$$\nabla \times \mathbf{E} = -\frac{\partial \mathbf{B}}{\partial t} \quad (6)$$

$$\nabla \times \mathbf{H} = \mathbf{J} + \frac{\partial \mathbf{B}}{\partial t} \quad (7)$$

And the constitutive relations in linear and isotropic medium (8), (9) and (10).

$$\mathbf{D} = \varepsilon \mathbf{E} \quad (8)$$

$$\mathbf{B} = \mu \mathbf{H} \quad (9)$$

$$\mathbf{J} = \sigma \mathbf{E} \quad (10)$$

These equations can be simplified by assuming time harmonic variables with radian frequency ω, (6) and (7) can be written as (11) and (12) respectively.

$$\nabla \times \mathbf{E} = -j\omega\mu \mathbf{H} \quad (11)$$

$$\nabla \times \mathbf{H} = (\sigma + j\omega\varepsilon)\mathbf{E} + \mathbf{J}^s \quad (12)$$

$\mathbf{J}^s$ is the source current. The expression for **E** given in (11) can be rewritten as (12) where ψ is the scalar electric potential and **A** is the magnetic vector potential.

$$\mathbf{E} = -\nabla\psi - \frac{\partial \mathbf{A}}{\partial t} \tag{13}$$

If magnetic induction of electric field is neglected compared to the spatial gradient of the potential ψ, then the equation holds for the quasi-static case and (13) can be reduced to (14).

$$\mathbf{E} = -\nabla\psi \tag{14}$$

By taking the divergence on both sides of (12) and substituting (14) into (12) we get (15).

$$\nabla \cdot (\sigma + j\omega\varepsilon)\nabla\psi = 0 \tag{15}$$

The potential function ψ is a function of σ and ε and these are functions of position, we assume time invariance.

Several different boundary condition models are used and they give different results:

- Continuum model – Assumes that there are no electrodes and the injected current or applied voltage is a continuous function of position on the surface boundary of the imaging domain.
- Gap model – Assumes uniform distribution of injected current or applied voltage under each electrode. Elsewhere on the boundary the currents and voltages are zero.
- Shunt model – Takes into account the shunting effect of the electrode i.e. assumes that the potential under each electrode is constant.
- Complete electrode model – Takes into account the shunting effect of the electrode as well as the impedance between the electrode and the tissue at the point of contact.

The image is built by comparing the measured boundary data values with the calculated model boundary data values and by minimization of the error function χ^2 given in (16).

$$\chi^2 = \sum_{i=1}^{O_{IM}} \left(\phi_i^m - \phi_i^c\right)^2 \tag{16}$$

The distribution of σ and ε that minimizes χ^2 provides the image of the objects electrical properties. It has been shown that a trigonometric excitation pattern provide the maximum sensitivity to structural heterogeneity for a cylindrically symmetric geometry. This means that voltages or currents that follow trigonometric functions of different frequencies are applied in sequence to the electrodes around the perimeter of the object. Only functions with integer number of half periods are used. Qualitative measurements of the complex conductance "map" have shown that you obtain a low conductivity halo around the periphery of the image and also a bad approximation of the global conductivity average in the object. This is counteracted by more accurately modelled electrodes and by data calibration to a known model of the test object. For simple experimental phantoms this has been a successful way but if it is to be performed for a real breast examination, an appropriate reference model of the breast must be made. So far only 2D reconstruction has been performed in practice but the group has shown the ability to 3D reconstructions with computer simulations of a 3Dcylinder equipped with layers of electrodes. The image reconstruction is built on the assumption that the induced currents only flow in the imaging plane, this is clearly not true for current propagation in a complex structure as the breast. Objects that don't intersect the imaging plane will interact with the applied currents and affect the measurements made in the plane. This is true for both the 2D reconstruction technique as well as for the 3D reconstruction technique that is built as a combination of multiple planar 2D arrays. Three generations of systems for in vivo measurements have been built and the last one is highly complex system build with layers of planar arrays that are adjustable to fit different breast sizes. A cylindrical geometry of each layer is obtained through slight compression of the breast but no discomfort is reported. No measurement data for real measurements with the third generation system is reported but some results from measurements on phantoms are shown. The conclusion is that EIS will never be able to compete with X-ray tomography methods for image resolution. The results show, however, that the method is more specific in discriminating between certain types of soft tissues, specifically in showing large contrast for malignant breast tissues as compared to normal tissues or fat. The method is seen as a complement to X-ray mammography for the above mentioned application.

MIS – Microwave Imaging Spectroscopy

The magnetic permeability is effectively uniform in the body but the permittivity and the conductivity vary locally mainly depending on the water and/or fat content in the tissue. As referred to in the EIS-part, these parameters will have a large contrast between malignant tissues compared to normal, healthy breast tissues. In this case the frequencies are higher but the contrast is still high. Two types of the method can be used, backscatter or transmission (for more information see Uppgift 3). The group uses the transmission method. As before the computer model (forward solver) is based on the Finite Element (FE) method but this time together with the Boundary Element (BE) method. The forward solver is a hybrid FE and BE method and it solves

Maxwell's equations (see part about EIS) in 2D. The FE-region is used to describe the imaging zone including the antennas and the BE-region is the un-bounded region outside the FE-region. The BE-region is filled with a liquid coupling medium sufficiently lossy enough to minimize the reflection effects from the surroundings. This medium is also used to couple the energy into the body without large reflections from the skin interface. The antennas used must therefore be suitable for immersion in this medium and "modellable" in the used forward solver. The result of the forward solver is compared with the measured field and the model is optimized with a Gauss-Newton Iterative reconstruction algorithm until the correct distribution of the electrical properties of the object is found. The group uses simple monopole antennas because they are easy to model accurately, they occupy a small volume which makes it possible to use many antennas and when placed in saline they show a broad bandwidth and fairly good (-10 dB) Return Loss (RL) in the given frequency range of interest (100 MHz-1100MHz). In order to reduce mutual coupling between antenna elements in the monopole array, each non-active antenna element is terminated with a matched load impedance. Different methods have been proposed to find the actual contour of the breast, both methods that include extra hardware like optical lazer or ultrasound measurements and methods that calculate the boundaries from the measured data have been used. A superheterodyne approach is used to recover the coherent signals required for the reconstruction algorithm. Carrier frequencies between 500 and 3000 MHz has been used and IF of 1 MHz or less make sure that excellent phase and amplitude detection can be made with relatively low cost components. Phase and amplitude data are collected both with and without an imaging target present so that the scattered fields for each measurement can be recovered by simple log-magnitude and phase subtractions. The number of channels used in the measurements varies from system to system. The simplest but slowest is when you have a mobile transmit and a mobile receive antenna that are placed in different positions to create a lot of measurement points. A faster way is to implement an array of antennas that also can be moved but this causes antenna interaction effects. The antennas must be separated enough to reduce interaction but be tight enough to increase resolution. The group has chosen a circular ring of 16 vertically oriented monopole antennas that can be moved in the vertical direction to collect data in different planes and create 3D solutions. Their system can handle 32 (so far only 16 is used) channels and include sophisticated switching devices. One antenna at the time acts as a transmitter and the other 15 as receivers. A separate receiver for every channel is used to exploit the parallel data acquisition capabilities and to minimize channel-channel crosstalk. But studies on phantoms and in vivo studies have been performed with this system and shows promising results.

NIR – Near Infrared Spectroscopy Imaging

As early as the 1920's tumours where being examined with red light transmitted through the breast. Laser scanning equipment was commercialized even before it's medical efficacy was established and studies in the US and Sweden showed that the method was not as sensitive as mammography when it comes to detecting smaller lesions in the breast. The method of NIR spectroscopy however became very successful and is widely used today for measuring arterial oxygen saturation from, for example, blood flow in the finger, toe or earlobe.

The diffusion equation is used in the forward solver, the equation is applicable when the method is applied to tissues in which scattering dominates absorption and the point of measurement is more than a few scattering lengths from the point of illumination. (In tissue, more than about 3mm.) The choice of boundary condition at the tissue surface is an issue of particular interest. Two assumptions has been made to simplify the diffusion equation:

- The radiance is only linearly anisotropic
- The rate of change of the flux is much lower than the collision frequency

Further they also assume that the radiance in tissue can be represented by an isotropic fluence rate plus a small directional flux. FEM is used to solve the diffusion equation in the image area and the Levenberg-Marquart algorithm is used to solve the optimization problem. When solving the problems a-priori information about the optical properties of the tissue is used, this information is obtained with MRI. Images from simulations have shown that the system can distinguish between absorption anomalies and scatter anomalies, at least when they are placed close to the source or receivers. The clinical studies using NIR has used the multi spectral approach to find the levels of haemoglobin, oxygen saturation and water content in the different regions throughout the breast. Also the total absorption coefficient for different wavelengths has been measured and in vivo measurements clearly shows tumour occurrence as increased absorption, increased total haemoglobin and water content. Also images showing the scattering coefficient show the anomaly as an abnormal scattering value even though the result is less clear compared to the absorption graphs. The system used is based on a diode laser coupled via fibre optical cables fed via a filter wheel to a multiplier tube. The received signal is measured at one point at the time with the help of a linear translation stage. Calibration of the system is performed with well known, homogenous reference objects.

Summary of Uppgift 1

As far as I understand, the MRE and MIS seem to be the most promising methods while EIS and NIR suffer from bad resolution and poor penetration capabilities respectively. MRE uses MRI equipment to detect the difference in elastic properties of the imaging region which makes the technique rather expensive. Further the method need a large contrast or large sized tumours before they can be detected with the method. The MIS method is able to obtain good resolution with many measurement points and is able to penetrate the breast deep enough to find tumours hidden deep into the breast tissue. A problem of the method seems to be how to couple the energy effectively into the breast and to find the appropriate antenna type. Also the measurement time seems to be a bit too long for a clinical system at least if we want to obtain good resolution with many measurement points. Some suggestions on how to overcome these problems with MIS is given in Uppgift 4.

Uppgift 2

Unwrapping of phase and the log-magnitude method are needed because two measurements are performed for each object. First a measurement without the object is performed and later on a measurement with the object present is done. By using the log-magnitude a simple subtraction can be performed on the results of the magnitude measurements for the both cases. The phase unwrapping is needed because the relative phase difference between two receive antennas can sometimes be larger than π rad or 180 degrees which causes problems since the phase is a periodic function. An example would be that the actual phase difference between two antennas is 380 degrees but by looking at the phase in the "periodic format" it would appear to be 20 degrees. Therefore one needs to map each phase value on to the correct Riemann sheet. The phase wrapping is more severe for widely spaced measurement points than for closely spaced ones and also the wrapping occurs more frequently for image objects with a large contrast in dielectric properties. In order to cope with the problem a phase unwrapping must be performed. In this case a simulation study is made of the object "octagon" in Qwed. The object is an octagonal metallic cavity with three ports (antennas) that can couple energy into or out of the cavity. One antenna is used as transmit and the other two as receive according to the figure below.

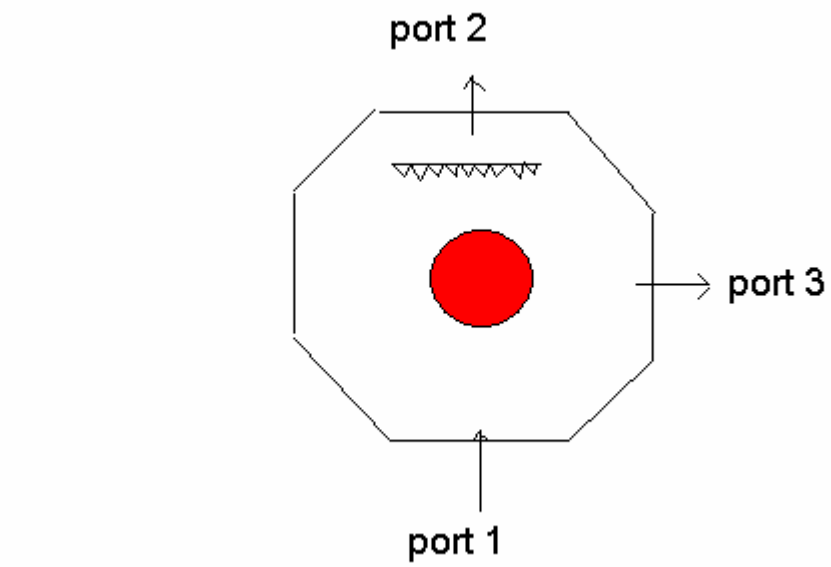

The cavity is filled with water and a cylinder of blood is located in the middle of the cavity also in this case an absorbing wall is modelled to reduce the direct connection between port 1 and port 2. The individual and differential phase of the signals in port 2 and 3 are shown in the figures below. In all plots the x-axis is the frequency in GHz and the y-axis is the phase in degrees.

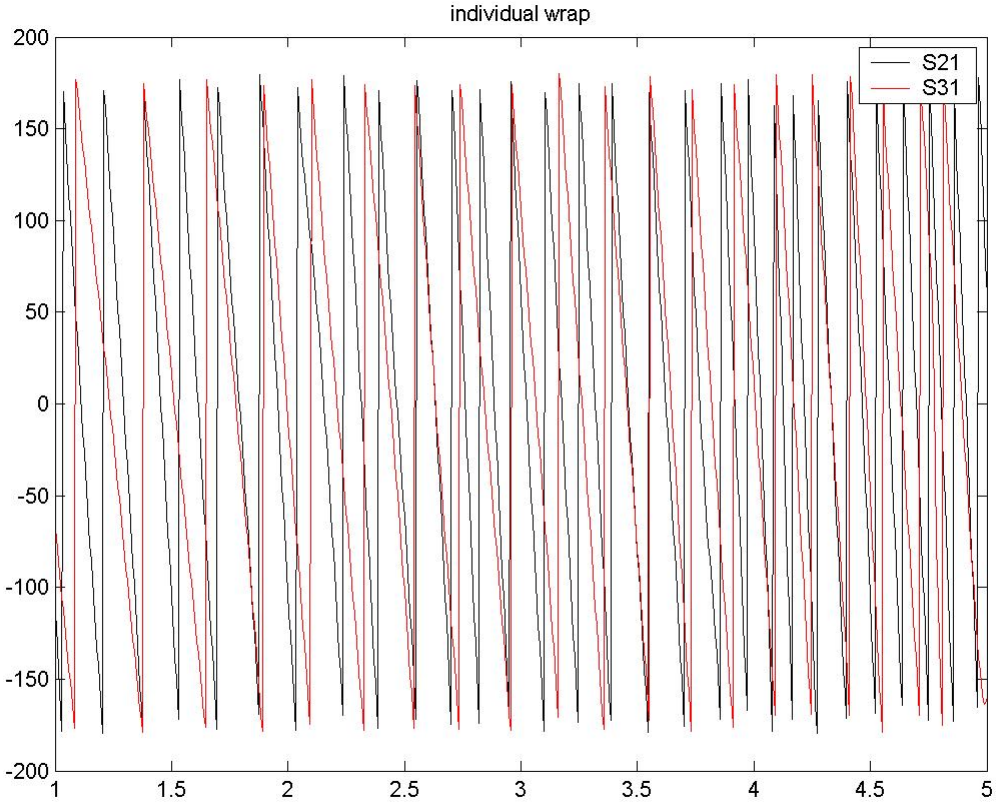
individual wrap
S21
S31
200
150
100
50
0
-50
-100
-150
-200
1
1.5
2
2.5
3
3.5
4
4.5
5

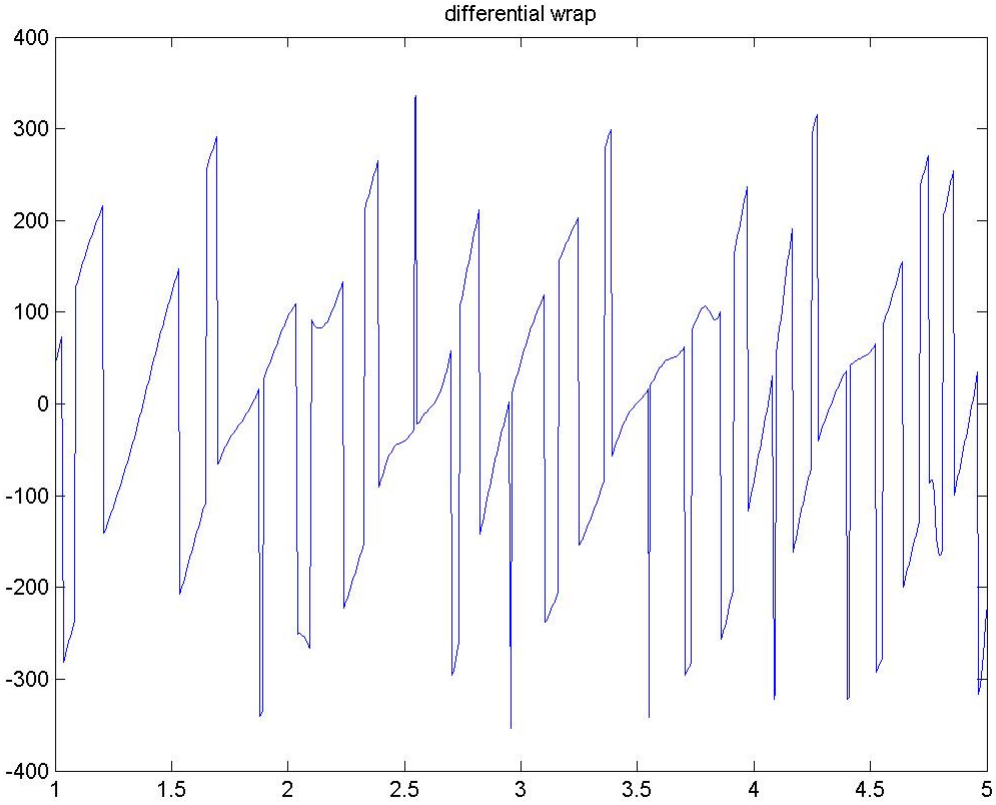
differential wrap
400
300
200
100
0
-100
-200
-300
-400
1
1.5
2
2.5
3
3.5
4
4.5
5

As one can see the differential phase varies very quickly with jumps where the individual phases shifts from -180 degrees to 180 degrees. If we map the phases into different Riemann sheets the plots will be as below and this is the unwrapped phases and their difference.

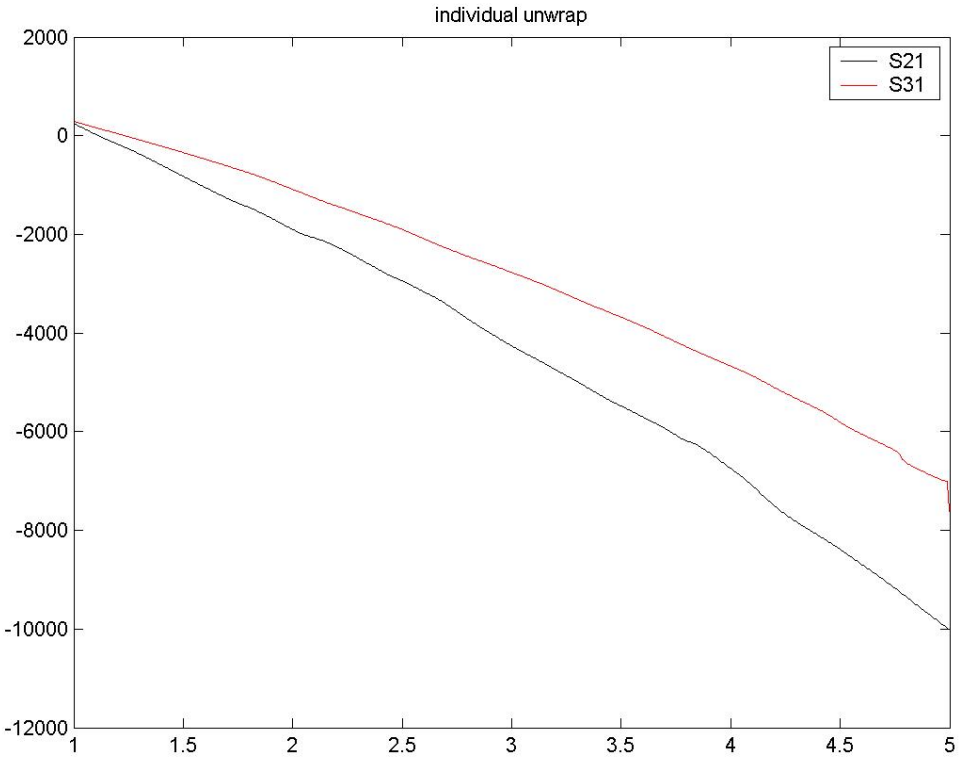

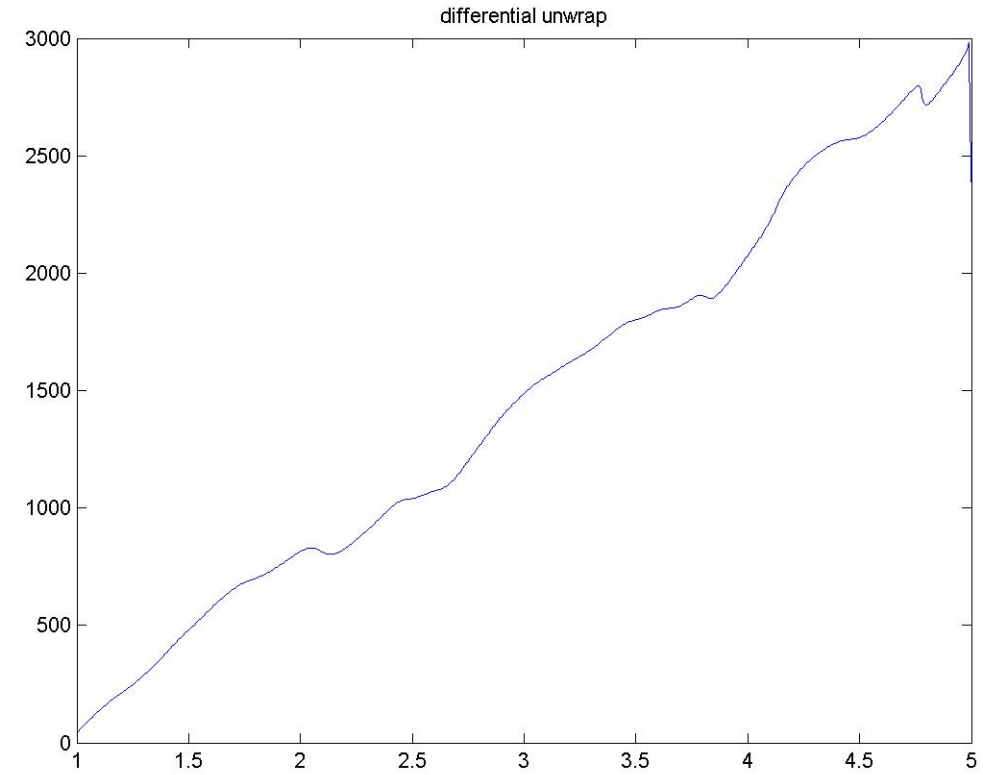

The "trick" is to lower the frequency until the phase is no longer wrapped and then keep record of the number of wrappings that occur when you increase the frequency to be able to map the phase values on to the Riemann

sheets. One more interesting thing is the sudden jumps in the individual values of the unwrapped phase and of course also in the differential value. One can see such a jump in the very end of the graphs above but more clearly in the graphs below. This time the octagon is modelled without the absorbing wall but still a cylinder of blood and also without the wall and with a cylinder of air.

For blood cylinder without the absorbing wall

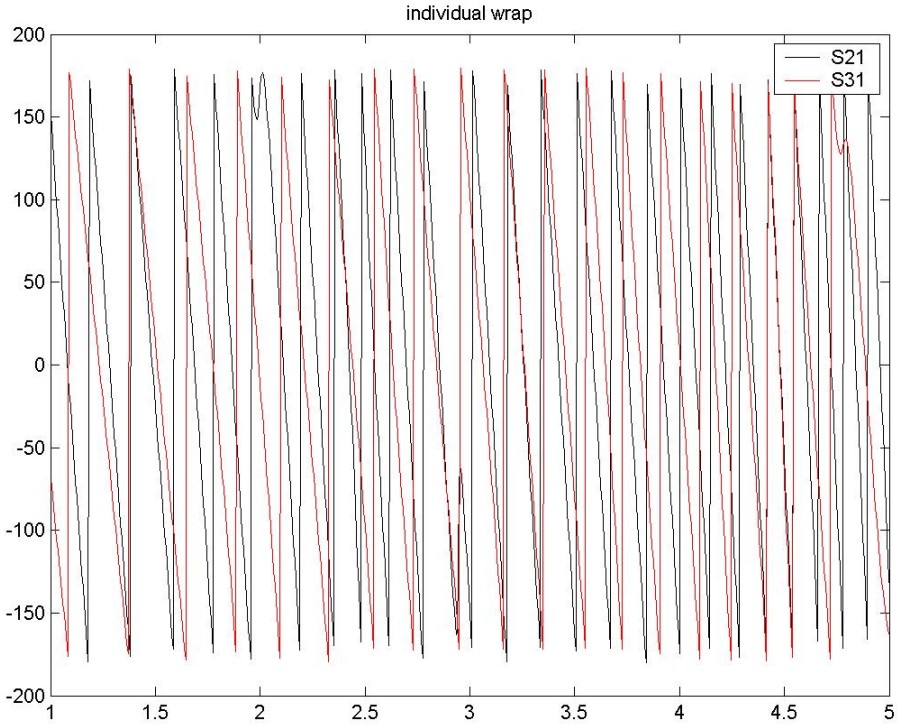

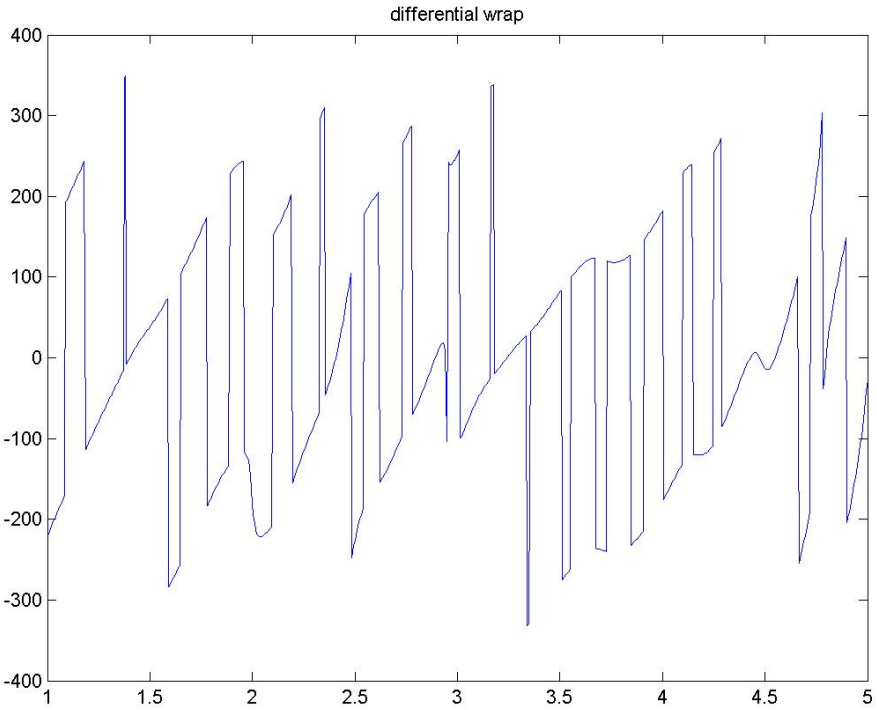

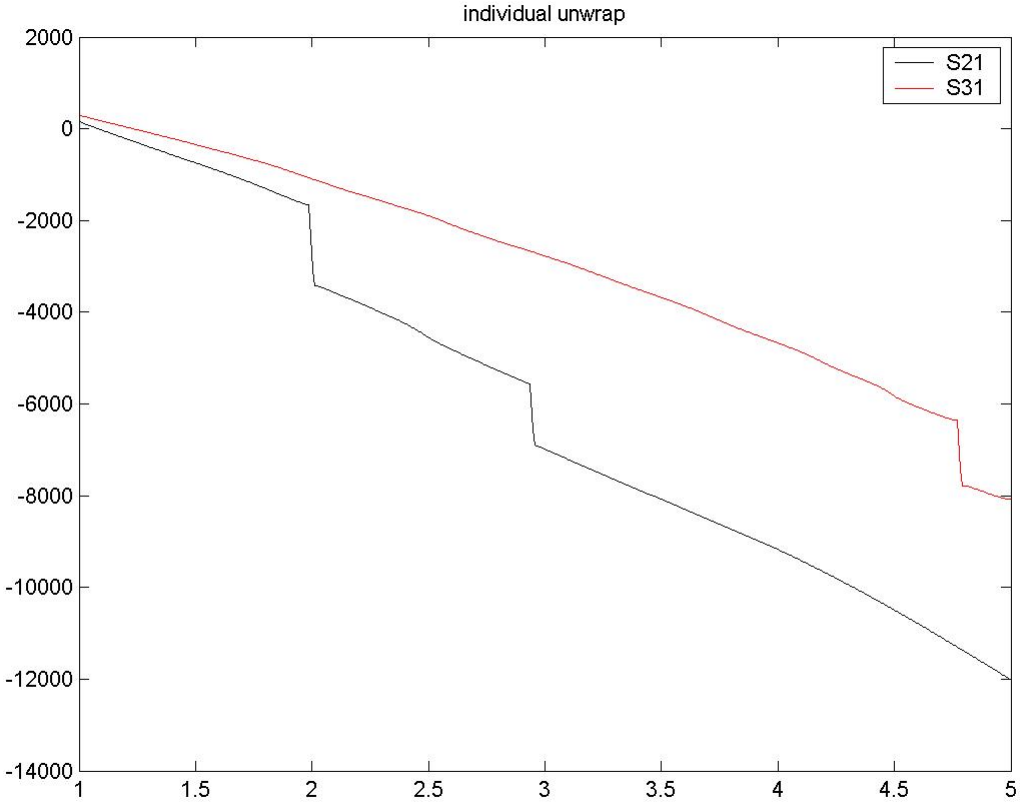
individual unwrap
S21
S31
2000
0
-2000
-4000
-6000
-8000
-10000
-12000
-14000
1
1.5
2
2.5
3
3.5
4
4.5
5

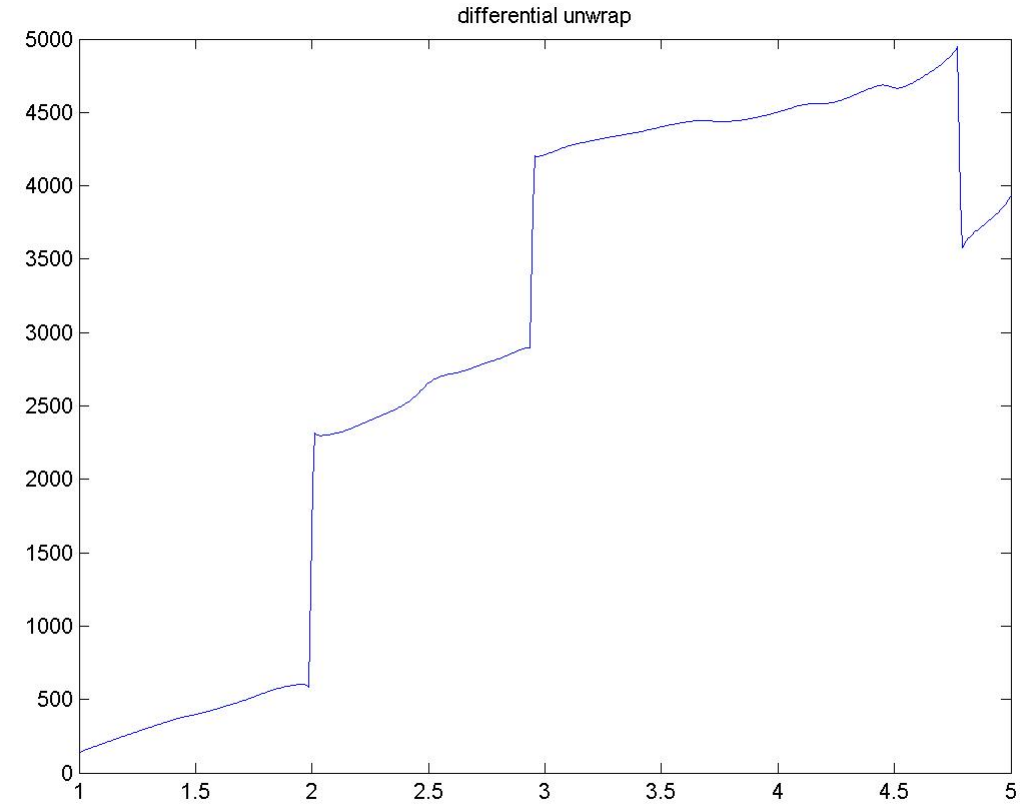
differential unwrap
5000
4500
4000
3500
3000
2500
2000
1500
1000
500
0
1
1.5
2
2.5
3
3.5
4
4.5
5

Air cylinder without absorbing wall

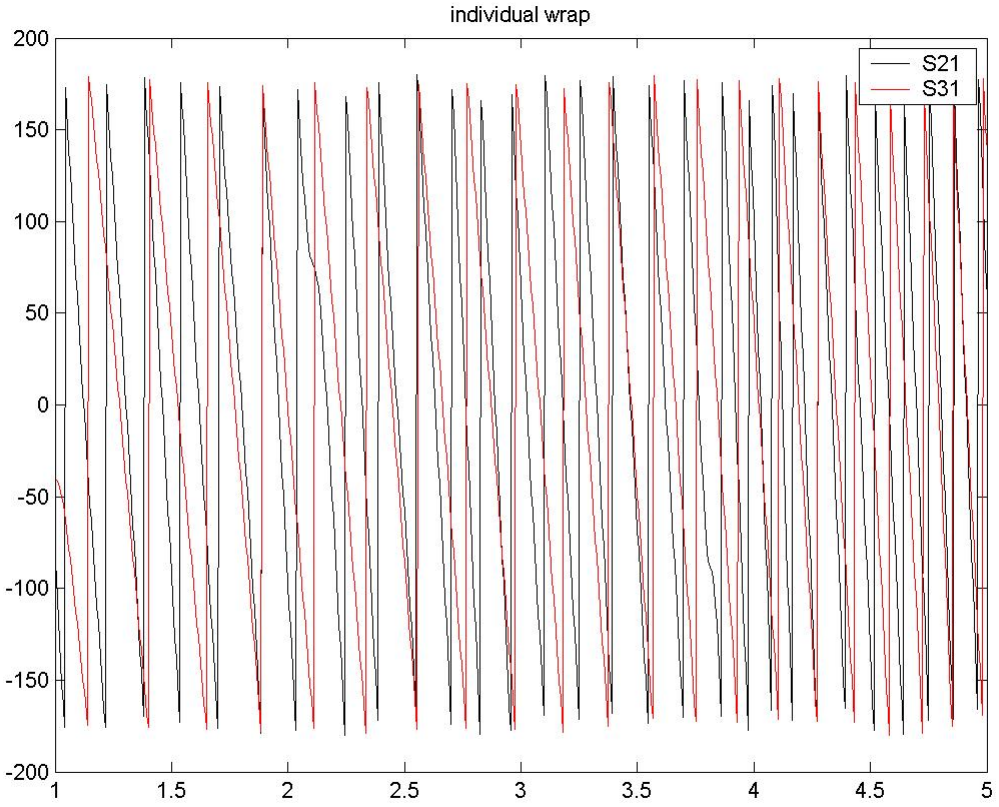

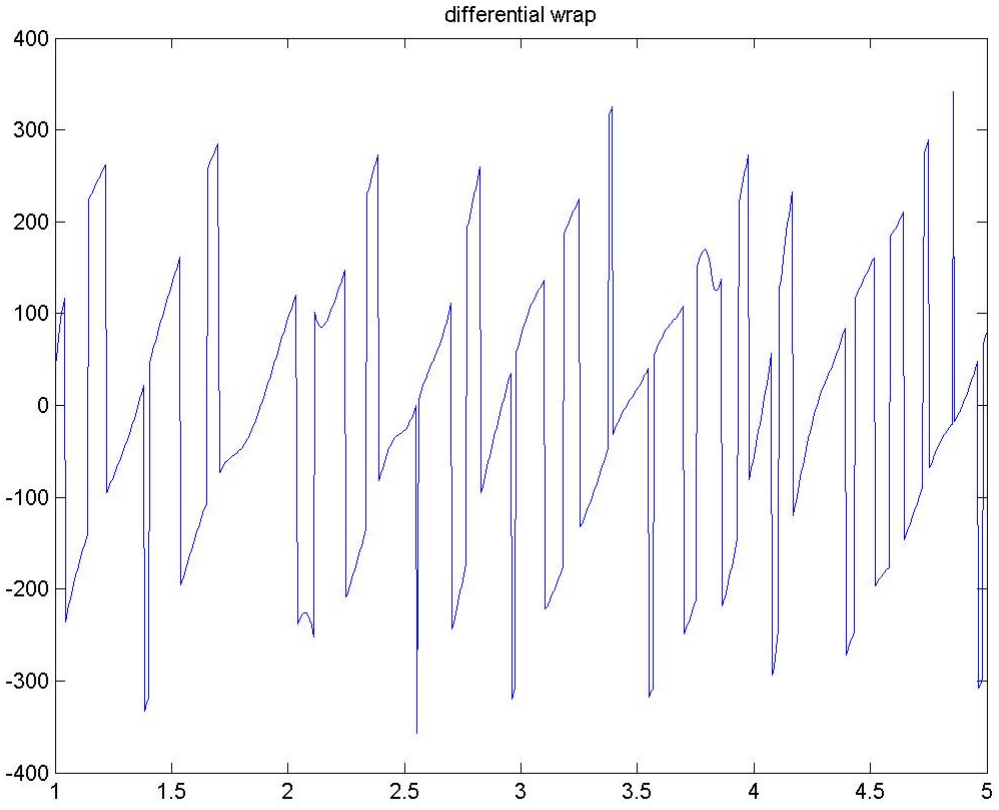

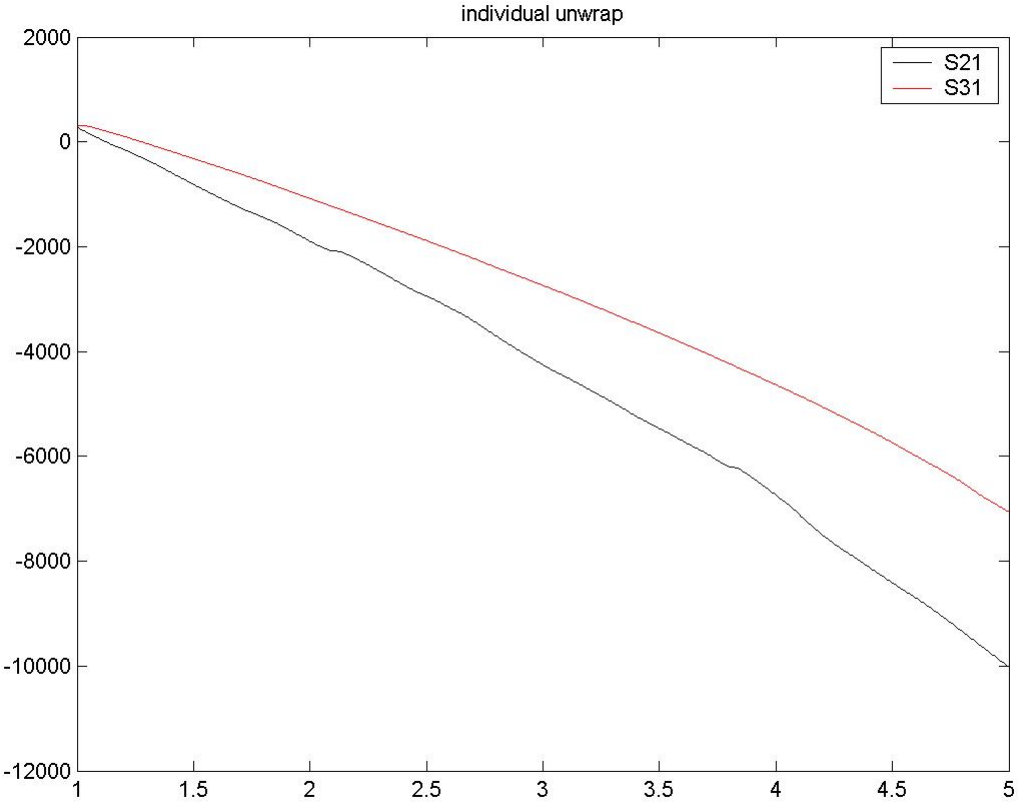
individual unwrap
S21
S31
2000
0
-2000
-4000
-6000
-8000
-10000
-12000
1
1.5
2
2.5
3
3.5
4
4.5
5

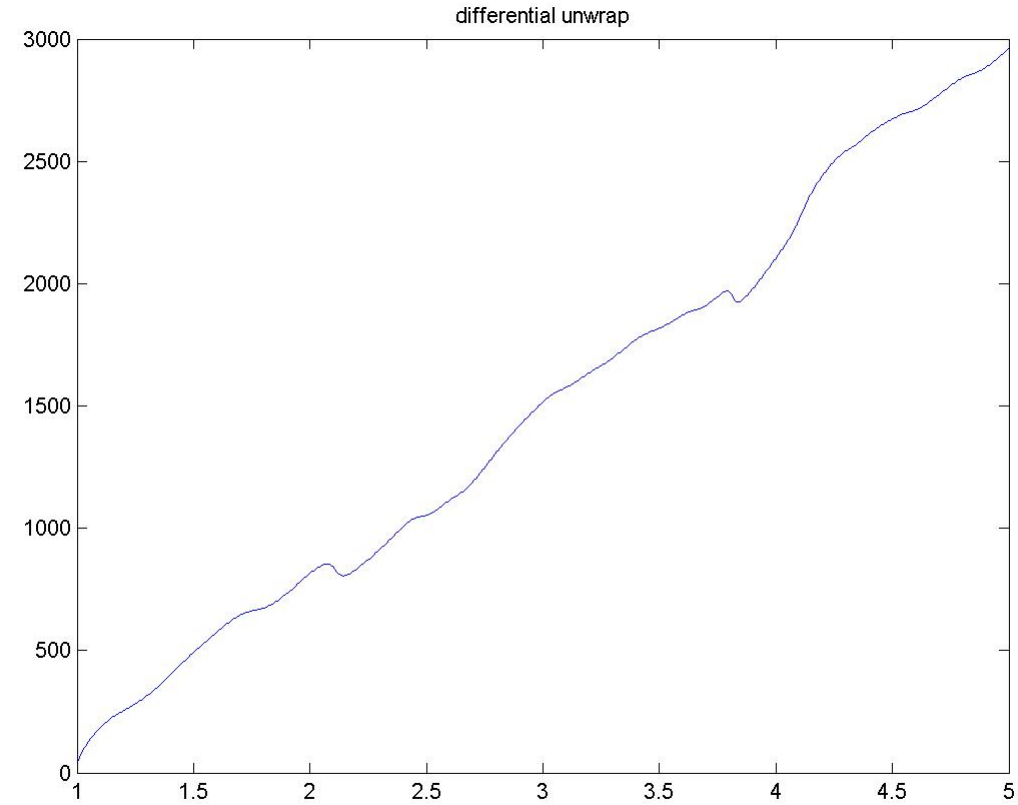
differential unwrap
3000
2500
2000
1500
1000
500
0
1
1.5
2
2.5
3
3.5
4
4.5
5

The sudden jumps, especially shown in the case for the blood cylinder without the wall, could be due to something like the "scattering null". If a scattered signal is approaching zero amplitude the phase state of the signal becomes undefined i.e. a vector of length 0 has no phase angle. In such a case the phase angle could be given any number and therefore a sudden jump might occur in the otherwise continuous graph. A recent article by Fang, Meaney and Paulsen "The Multidimensional Phase Unwrapping Integral and Applications to Microwave Tomographical Image Reconstruction" published in IEEE Transactions on Image Processing is dealing with this problem with scattering nulls and suggests a method to overcome the problem.

Uppgift 3

I will focus on the hardware differences since this is my area of interest. There are differences in the algorithm part of the problem as well but this is another area and will not be discussed here.

The group of Semenov uses the same basic wave propagation technique to create the image as Paulsen and Meaney. Both groups use the transmitted, scattered fields to build an image of the internal of the imaging object. Semenov uses frequencies from 900 MHz up to just above 2 GHz and Paulsen and Meaney has built their system for frequencies from 500 MHz up to 3 GHz, although the practical results that they show is for frequencies around 1 GHz. Semenov's system has flexible antenna positioning with robot control of both the transmit and receive antenna. In this way a flexible number of positions in 3D can be measured both for the transmit and the receive antenna but since the measurements must be performed in series the measurement time is extremely high for a large number of positions. A Network Analyzer is used to transmit and detect signals this is to be compared with Paulsen and Meaney's traditional radio receiver technique used for signal detection. The network analyzer will easily provide the amplitude and phase of the scattered signals and Semenov has also combined it with the possibility to rotate the antennas in order to measure different polarizations. The antennas are open waveguide antennas filled with high ε dielectric material, to reduce the edge effects the open waveguides are placed on large groundplanes. The choice of coupling medium is also different for Semenovs group compared to Paulsen and Meaney, Semenov used a saline solution with approximately $\varepsilon=79+j10$ over the used frequency band. Paulsen and Meaney uses for example a glycerine-water solution with real part of ε between 10 and 25 typically. Semenovs group was the first to conclude that building a 3D image from 2D slices is not possible, the need of a full 3D simulation is necessary to obtain a good 3D image of the object.

The group of Hagness use a radar back scattering technique to detect tumours. The difference in dielectric properties of the tumour compared to healthy tissue is expected to create a difference in radar cross section. The group uses an UWB technique with frequencies around the same values as the other groups, in practice the large part of the power is located in the band 500 MHz to 2.5 GHz. FDTD simulations are used as the numerical tool and the parameters of the Debye dispersion equation are estimated from the simulations and measurements to find the dielectric property distribution of the imaging region. The group uses a single broadband horn antenna placed at different locations to excite and measure the scattered field. The horn antenna is filled with a dielectric (oil) with $\varepsilon_r=2.6$ and $\sigma=0.05$ S/m to act as a coupling medium between the antenna and the body. In the calibration procedure a measurement is done with the test object to estimate the average value of the dielectric constant for the imaging volume. In this calibration the imaging object is considered as two homogenous regions, the skin and the underlying tissue which will reduce the number of unknowns in the inverse problem.

Uppgift 4

In order to develop the "ultimate tomography equipment" for breast cancer detection at Mälardalen University, there are some questions that must be answered.

First the question of the coupling medium:
Why does every group use different kinds of coupling mediums? The mediums are not just of different types but also diverge a lot in dielectric properties. Some tries to model the same properties as fatty breast tissue but isn't the skin properties of larger interest since this is the first interface that the waves will meet? There will be a lot of other interfaces inside the breast but these will always be there and they will be out of our control. An investigation on how to maximize the energy coupled into the body must be performed and the proper choice of coupling medium must be done.
The coupling medium is also important when it comes to reflections from the surroundings. The medium should be lossy enough so that we can disregard any reflections from surrounding objects. Is there any other way to control these unwanted reflections? Do we need to include a lot of losses into the system just to control the environment outside the system? Is it possible to use some kind of mode stirring cavity in the system to control the reflections and be able to reduce or get rid of the unnecessary loss in the system?

The choice of proper antennas (sensors):
What is the optimum antenna to use in a system like this? Should it be a lot of antennas or just one that can be moved and create a flexible number of measurement/excitation points. What kind of antenna is suited for immersion into liquids (coupling mediums)? How do we match the antennas to the coupling medium instead of air? Can the antennas be placed directly onto the body and matched to the skin properties to be able to maximize the energy coupled into the body? Is the Modulated Scatterer Technique suitable for detection or should a more traditional radio receiver technique be used? Do we need a broadband system or is it sufficient with a narrow band system? In the narrow band approach, should we use multiple frequencies or try to find the optimum frequency for the breast cancer application?

Can AI be used in some step of the process? Either for pure image quality enhancement or more integrated in the optimization process of the inverse problem.

There are a lot of research questions to be answered and some interesting threads to follow!

As a first step the tomograph at Mälardalen University will use a robot to control the measurement points and water will be used as coupling medium. Water is easy to access and has well known dielectric properties. A simple monopole antenna array is available for initial experiments and we plan to build a “retina” using the Modulated Scatterer Technique in order to use the experience from Supélec, Paris and their planar microwave camera.